

New type of olivine fabric from deformation experiments at modest water content and low stress

Ikuo Katayama

Department of Geology and Geophysics, Yale University, New Haven, Connecticut 06520, USA

Haemyeong Jung

Institute of Geophysics and Planetary Physics, University of California, Riverside, California 92521, USA

Shun-ichiro Karato

Department of Geology and Geophysics, Yale University, New Haven, Connecticut 06520, USA

ABSTRACT

A new type of olivine fabric was found by high-strain simple-shear deformation experiments in the presence of trace amounts of water at $\sim 0.5\text{--}2.2$ GPa and $\sim 1470\text{--}1570$ K. In this fabric, called E-type fabric, the olivine [100] axis is subparallel to the shear direction, and the (001) plane is parallel to the shear plane; this geometry suggests that the [100](001) slip system makes the dominant contribution to total strain. This fabric is dominant at a modest water content, $200 < C_{\text{OH}} < 1000$ H/10⁶Si at low stresses and high temperatures. Some mylonites from peridotite massifs show this type of olivine fabric, which suggests the presence of water during the shear localization. The seismic anisotropy caused by this fabric is qualitatively similar to that by dry fabric (A type), but the magnitudes of anisotropy are different between the two types: for horizontal flow, the amplitude of $V_{\text{SH}}/V_{\text{SV}}$ anisotropy is weaker, but the amplitude of shear-wave splitting is stronger for the E-type fabric than for the A-type dry fabric. Seismic anisotropy in the oceanic upper mantle may be due to the olivine E-type fabric.

Keywords: lattice-preferred orientation, olivine, water, deformation, seismic anisotropy.

INTRODUCTION

The relationship between lattice-preferred orientation (LPO) and flow geometry has important applications for the interpretation of seismic anisotropy and the mechanisms of shear localization. The classic study by Carter and Avé Lallemant (1970) showed that olivine deformation fabrics, which are controlled by dominant slip systems, depend on the physical condition of deformation, particularly the strain rate (stress magnitude) and temperature. Jung and Karato (2001a) extended this work and found that in addition to these physical variables, water has important effects on olivine fabric; they reported two new types of fabrics called B- and C-type fabrics. In these fabrics, the olivine [001] axis is subparallel to the shear direction, the (010) plane is subparallel to the shear plane (B type), and the (100) plane is subparallel to the shear plane (C type). We have conducted new deformation experiments to define the boundaries between the different fabrics and discovered a new type of olivine fabric developed under conditions of modest water content, which we call E-type fabric. In this fabric, the olivine [100] axis is subparallel to the shear direction, and the (001) plane is parallel to the shear plane; this geometry suggests that the [100](001) is the dominant slip system. Here we report characteristics of this new olivine fabric and dis-

uss its implications for seismic anisotropy and the shear localization in naturally deformed peridotites.

EXPERIMENTAL TECHNIQUE

We conducted deformation experiments in simple-shear geometry at temperatures of 1470–1570 K and pressures of 0.5–2.2 GPa by using a solid-medium apparatus (Griggs type). We used San Carlos olivine single crystals oriented [100] parallel to the shear direction and [001] normal to the shear plane, or hot-pressed olivine aggregates as starting materials. An olivine sample was sandwiched between alumina pistons, cut at 45° from the maximum compression direction, and was surrounded by a mixture of talc and brucite that acted as a water source (Fig. 1). Pressure was first raised to a desired value, and then temperature was increased at a rate of ~ 30 K/min, which was monitored by using Pt/Rh thermocouples inserted into the cell assembly. After the temperature was stabilized, a piston was advanced at a constant rate. To produce modest water content, two alternative methods were used: (1) by adding silica to the talc and brucite mixture to decrease the mixture's melting temperature, the water released is mostly partitioned to the melt layer, or (2) by doing experiments at lower pressure (~ 0.5 GPa) at which the water solubility in olivine is signif-

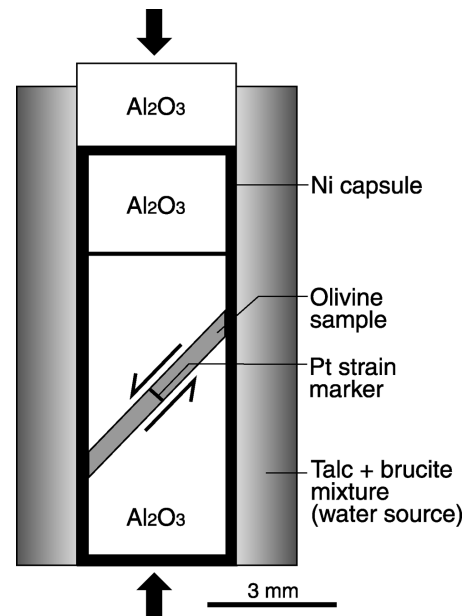


Figure 1. Experimental cell assembly for simple-shear deformation. Water was supplied by breakdown of talc and brucite mixture at high temperatures. Thin platinum-coated layer was inserted in olivine sample, and strain was measured by rotation of this layer.

TABLE 1. EXPERIMENTAL CONDITIONS AND RESULTS

Run no.	Pressure (GPa)	Temperature (K)	Shear strain (γ)	Strain rate (s^{-1})	Stress* (MPa)	Water content† (H/10 ⁶ Si)	Final grain size (μm)	Fabric type
GA10	2.0	1470	0.6	8.3×10^{-5}	270	540	15	E#
GA12	2.0	1470	1.2	5.7×10^{-5}	230	560	19	E
GA23	2.0	1470	0.8	5.0×10^{-5}	190	630	37	E
GA25	2.0	1470	6.3	1.6×10^{-4}	320	280	10	E
GA38 [§]	0.5	1470	0.6	3.1×10^{-5}	190	210	16	E
GA45 [§]	0.5	1470	2.6	1.5×10^{-4}	300	330	8	E
JK12	2.2	1570	1.0	1.0×10^{-4}	250	800	23	E#
JK30	1.0	1470	1.1	5.5×10^{-4}	250	650	10	E#
JK47	0.5	1570	0.7	1.1×10^{-4}	110	400	14	E

*Differential stress was calculated from dislocation density of deformed olivine samples; see detail in Karato and Jung (2003).

†Water content of olivine crystals was measured by Fourier transform infrared (FTIR) spectroscopy using a calibration of Paterson (1982).

§Starting material was hot-pressed olivine aggregates. Single-crystal olivine was used for the other experiments.

[100] maximum in these samples is significantly deviated from the shear direction (refer to open symbols in Fig. 4).

icantly lower (Kohlstedt et al., 1996). After the experiments, the olivine samples were analyzed by Fourier transform infrared spectroscopy to quantify the water content. Water contents presented here were determined by the Paterson (1982) calibration. If the Bell et al. (2003) calibration is used, the results should be multiplied by a factor of ~ 3.5 . Shear strain was measured by the rotation of a platinum strain marker, which was initially oriented perpendicular to the shear direction. Solid-medium apparatus has a large friction component in the external load cell; therefore we used the dislocation density of deformed samples to infer the stress magnitude (Jung and Karato, 2001b; Karato and Jung, 2003). The microstructure and fabric of olivine samples were investigated by a scanning electron microscope equipped with an electron-backscatter diffraction system.

RESULTS AND DISCUSSION

The results of experiments are summarized in Table 1. The samples were deformed, in approximately simple-shear geometry, to strains as high as $\gamma = \sim 6$. Even in cases where the starting material was a single crystal olivine, the recovered samples were totally recrystallized (Fig. 2A). The grains are characterized by mostly equal axes at relatively low strain, but show a slightly elongated grain shape at higher strain. The grain size varies from 10 to 37 μm , which shows a good correlation with the differential stress of deformed samples. We measured the water contents of the deformed samples and found that they contain 210–800 H/10⁶Si. The dislocations in the deformed olivine grains mostly have linear morphology (Figs. 2A, 2B); subboundaries are rare. However, in some grains we observe well-defined tilt boundaries (Fig. 2B) on the (100) plane where dislocation lines are along the [010] directions, suggesting that the [100](001) slip system makes a dominant

contribution. In addition, nearly straight dislocations are also observed in the [001] orientation, which are likely the screw dislocations with $\mathbf{b} = [001]$ (where \mathbf{b} is the Burgers vector).

Figure 3 shows the lattice-preferred orientation of the deformed olivine aggregates. In all cases the fabric is characterized by the [100] axis subparallel to the shear direction and the (001) plane subparallel to the shear plane, although the intensity of the fabric is substantially stronger when a single crystal was used as a starting material. We used single crystals of the same orientation in other experiments and obtained completely different fabrics (B type, C type) under different water content and stress conditions. Consequently, we conclude that although the orientation of the starting single crystal has some effects on fabric strength, the initial orientation does not change the geometry of the fabrics. This result is distinct from previously reported olivine fabrics from experimental studies. In the earlier-reported fabrics under dry conditions, the [100] axis is subparallel to the shear direction, and the (010) plane (A type) or the $\{0kl\}$ plane (D type) is subparallel to the shear plane (Zhang and Karato, 1995; Bystricky et al., 2000). In the earlier-reported fabrics under water-rich conditions, the [001] axis is subparallel to the shear direction, and the (010) plane (B type) or the (100) plane (C type) is subparallel to the shear plane (Jung and Karato, 2001a). This new olivine fabric we call E type.

In the E-type fabric, the [100] peak is nearly parallel to the shear direction, but, in samples with higher water content close to the transition between E and C types, the orientation maximum is significantly deviated from the shear direction. This deviation is probably due to the concurrent operation of the [001](100) slip system (C-type fabric), which is also suggested by the dislocation microstructures of

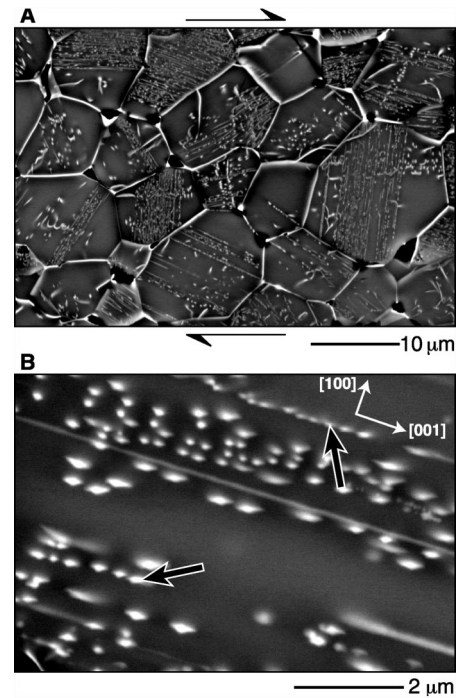


Figure 2. A: Backscattered-electron image of deformed sample (GA12) after oxidation at 1073 K for 1 h. Bright lines or dots within olivine grains represent dislocations. Grain structures are characterized by mostly equal axis lengths in this sample ($\gamma = \sim 1.2$), and dislocations are mostly straight. Thin arrows show sense of shear. B: Enlarged image of dislocation microstructures in deformed olivine crystals, showing tilt boundaries (thick arrows) on (100) plane where dislocation lines are along [010] directions.

the deformed olivine crystals (Fig. 2). In the dry fabric (A type), the [100] maximum is nearly parallel to the strain ellipsoids at lower strain and rotates toward the shear direction at large strains (Zhang and Karato, 1995). However, in the E-type fabric, the [100] peak is not parallel to the strain ellipsoids, which appears on the opposite side of the trace of the shear plane (Fig. 3). When a finite-strain ellipsoid is used as a reference frame for pole figures, then the relationship between the sense of shear and the position of peaks is similar between the A and E types. However, when the shear plane or shear direction is used as a reference frame (as in Fig. 3), then the relationship between the sense of shear and the position of poles is different between the two types of fabrics. Consequently, care must be used in inferring the sense of shear from the olivine fabrics.

The observed transition from A-type to E-type fabric is consistent with the results of an earlier study by Mackwell et al. (1985) in which the strength of olivine with the [101]_c orientation becomes comparable to that of the [110]_c when olivine is saturated with water at 300 MPa (Karato, 1995). This change indi-

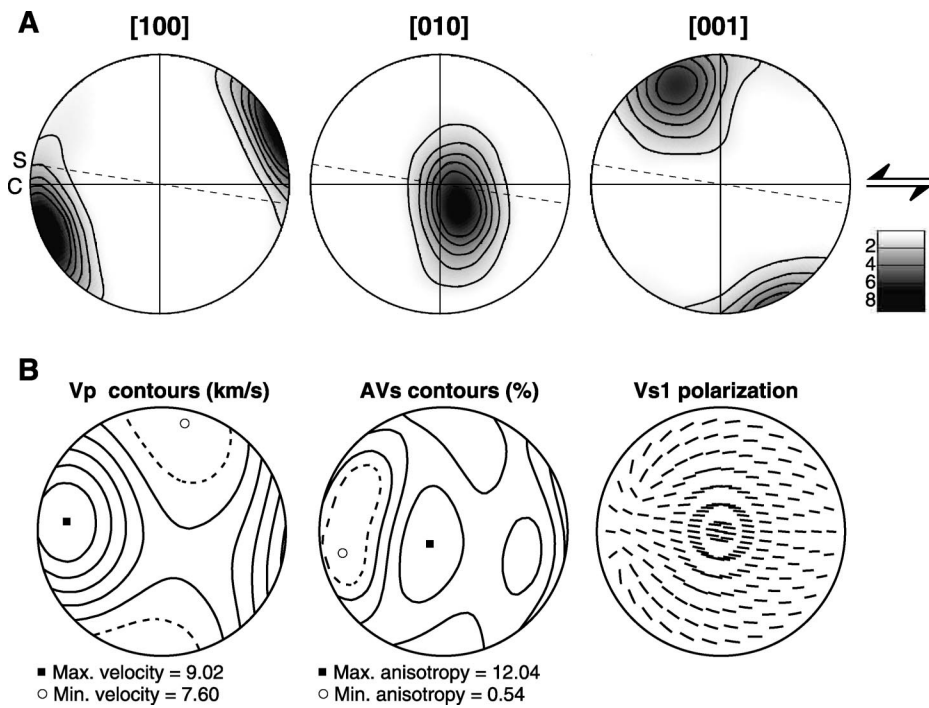


Figure 3. A: Pole figures of lattice-preferred orientation of deformed olivine aggregates (GA25). East-west direction corresponds to shear direction, and north (south) poles correspond to shear-plane normal. Dashed line represents trace of finite strain ellipsoid (S is maximum elongation direction and C is shear direction). Equal-area lower-hemisphere projection was used with half-width of 30° and contours at 2–8 multiples of random distribution. Orientations of total of 378 grains were measured. **B:** Seismic anisotropy for E-type olivine fabric calculated by using software of Mainprice (1990) from olivine aggregates plotted in A; these were calculated at 5 GPa and 1573 K. East-west direction corresponds to shear direction, and center of plot corresponds to shear-plane normal. Direction of maximum P-wave velocity and polarization of faster S-wave are subparallel to shear directions; this result is similar to result for A-type fabric, although amplitude of polarization anisotropy of S-wave on shear plane is much larger than that of A-type samples.

icates that deformation due to the [100](001) slip system is enhanced by water more than deformation by the [100](010) slip system and that the strength of these slip systems is comparable at the water content corresponding to the confining pressure of 300 MPa (~ 200 H/ 10^6 Si). Consequently, at higher water contents, the [100](001) slip system is likely to be easier than the [100](010) slip system, and hence the E-type fabric would dominate. This prediction is exactly what was found in this study. At higher water contents, yet another slip system, the [001](100) slip system, becomes easier and controls the fabric (C-type fabric). E-type fabric is therefore a dominant fabric at water contents of $200 < C_{OH} < 1000$ H/ 10^6 Si (Fig. 4). At higher stress, the [001](010) slip system becomes the dominant slip system (B type) at variable water contents (Jung and Karato, 2001a). Hence the E-type fabric is dominant at relatively lower stress, modest water contents, and high temperatures.

Most olivines from naturally deformed peridotites, including mantle xenoliths, show A-type dry fabric (e.g., Ben Ismail and Mainprice, 1998). However, B- and C-type wet fabrics have also been reported from some pe-

ridotites, particularly in plate-convergent regions where high water content is expected (e.g., Möckel, 1969; Frese et al., 2003; Mizukami et al., 2004). In addition, E-type fabric has also been documented in mylonites from the Bay of Islands ophiolite complex, Newfoundland (Mercier, 1985), and the Horoman peridotite complex, Japan (Sawaguchi, 2004). These mylonites are considered to have been formed during the emplacement of the peridotite massif into the crustal depths. The E-type fabric in such deformed peridotites suggests that aqueous fluids infiltrated and modified the olivine fabric during the shear localization. Similarly, Mehl et al. (2003) also reported E-type fabric from the Talkeetna arc complex in central Alaska and inferred a relatively high H_2O activity in the arc-subduction setting.

Elastic constants corresponding to E-type fabric (Table 2) were calculated from olivine polycrystal aggregates by using a Voigt-Reuss-Hill average. Seismological signatures of E-type fabric were computed by using the olivine elastic constants and are qualitatively similar to the characteristics of those of A-type fabric. The fast-propagation direction

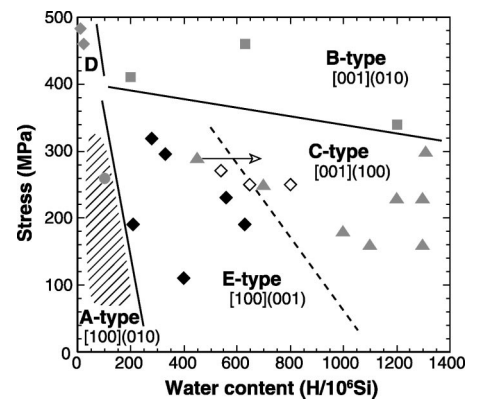


Figure 4. Olivine fabric diagram as function of stress (MPa) and water content (H/ 10^6 Si) at high temperatures ($T = 1470$ – 1570 K). Filled diamonds—E-type fabric; open diamonds—samples in which [100] maximum is significantly deviated from shear direction ($\sim 40^\circ$). Data for A, B, C, and D types (gray symbols and ruled area) are from Jung and Karato (2001a). Arrow indicates sample in which substantial amount of water has been lost during long deformation experiment. E type is dominant fabric at relatively lower stress and modest water content (at high temperatures).

(azimuthal anisotropy) and polarization of the faster S-wave are subparallel to the shear direction, and the horizontal shear causes $V_{SH} > V_{SV}$ (vertical: $V_{SH} < V_{SV}$) polarization anisotropy. However, the magnitudes of azimuthal anisotropy and shear-wave splitting for E-type fabric are apparently larger than those due to A-type fabric, and the V_{SH}/V_{SV} ratio (horizontal shear) is somewhat smaller. Seismic anisotropy in the oceanic mantle shows that the fast-propagation direction is nearly parallel to plate motion (e.g., Tanimoto and Anderson, 1984). This observation has been interpreted as indicating the presence of the olivine dry fabric (A type), in which the olivine [100] axis is subparallel to the flow direction and the olivine (010) plane is subparallel to the horizontal plane (e.g., Nicolas and Christensen, 1987). However, oceanic upper mantle is expected to contain a trace amount of water (~ 800 H/ 10^6 Si; Hirth and Kohlstedt,

TABLE 2. ELASTIC CONSTANTS (C_{ij}) OF OLIVINE E-TYPE FABRIC

i	$j = 1$	$j = 2$	$j = 3$	$j = 4$	$j = 5$	$j = 6$
1	258.1	79.0	87.3	-0.8	-13.8	-5.5
2		194.4	82.9	-1.7	2.1	-3.1
3			216.6	-1.9	-5.4	-1.3
4				60.9	-1.8	-2.9
5					76.2	0.4
6						67.8

Note: The C_{ij} (in GPa) was calculated from olivine aggregates (GA25) at 5 GPa and 1573 K. Pressure and temperature derivatives of the olivine C_{ij} values were taken from Abramson et al. (1997) and Isaak (1992), respectively. Reference axes defined as follows: 1—shear direction, 3—shear-plane normal, and 2—perpendicular to both 1 and 3 directions.

1996); hence the olivine deformation may be dominated by E-type fabric, rather than A-type dry fabric. Similar interpretation has also been proposed by natural E-type fabric in the Talkeetna arc complex (Mehl et al., 2003). Although the orientation of the fast-propagation direction alone cannot distinguish A- and E-type fabrics, the magnitudes of azimuthal and polarization anisotropies could help to infer the fabric in the oceanic upper mantle.

ACKNOWLEDGMENTS

We thank P. Skemer, Y. Nishihara, and K. Matsumage for discussion and Z. Jiang for technical assistance with electron backscatter diffraction analyses. Constructive comments by G. Hirth and an anonymous reviewer helped improve the manuscript. This study was supported in part by National Science Foundation grants (to Karato) and by a research fellowship of the Japan Society for the Promotion of Science (to Katayama).

REFERENCES CITED

- Abramson, E.H., Brown, J.M., Slutsky, L.J., and Zaig, J., 1997, The elastic constants of San Carlos olivine to 17 GPa: *Journal of Geophysical Research*, v. 102, p. 12,253–12,263.
- Bell, D.R., Rossman, G.R., Maldener, J., Endisch, D., and Rauch, F., 2003, Hydroxide in olivine: A quantitative determination of the absolute amount and calibration of the IR spectrum: *Journal of Geophysical Research*, v. 108, no. B2, 2105, doi: 10.1029/2001JB000679.
- Ben Ismail, W., and Mainprice, D., 1998, An olivine fabric database: An overview of upper mantle fabrics and seismic anisotropy: *Tectonophysics*, v. 296, p. 145–157.
- Bystricky, M., Kunze, K., Burlini, L., and Burg, J.-P., 2000, High shear strain of olivine aggregates: Rheological and seismic consequences: *Science*, v. 290, p. 1564–1567.
- Carter, N.L., and Avé Lallemant, H.G., 1970, High temperature deformation of dunite and peridotite: *Geological Society of America Bulletin*, v. 81, p. 2181–2202.
- Frese, K., Trommsdorff, V., and Kunze, K., 2003, Olivine [100] normal to foliation: Lattice preferred orientation in prograde garnet peridotite formed at high H₂O activity, Cima di Gagnone (Central Alps): *Contributions to Mineralogy and Petrology*, v. 145, p. 75–86.
- Hirth, G., and Kohlstedt, D.L., 1996, Water in the oceanic upper mantle: Implications for rheology, melt extraction and the evolution of the lithosphere: *Earth and Planetary Science Letters*, v. 144, p. 93–108.
- Isaak, D.G., 1992, High-temperature elasticity of iron-bearing olivines: *Journal of Geophysical Research*, v. 97, p. 1871–1885.
- Jung, H., and Karato, S., 2001a, Water-induced fabric transitions in olivine: *Science*, v. 293, p. 1460–1463.
- Jung, H., and Karato, S., 2001b, Effects of water on dynamically recrystallized grain-size of olivine: *Journal of Structural Geology*, v. 23, p. 1337–1344.
- Karato, S., 1995, Effects of water on seismic wave velocities in the upper mantle: *Japan Academy Proceedings*, v. 71, p. 61–66.
- Karato, S., and Jung, H., 2003, Effects of pressure on high-temperature dislocation creep in olivine: *Philosophical Magazine*, ser. A, v. 83, p. 401–414.
- Kohlstedt, D.L., Keppler, H., and Rubie, D.C., 1996, Solubility of water in the α , β and γ phases of (Mg,Fe)₂SiO₄: *Contributions to Mineralogy and Petrology*, v. 123, p. 345–357.
- Mackwell, S.J., Kohlstedt, D.L., and Paterson, M.S., 1985, The role of water in the deformation of olivine single crystals: *Journal of Geophysical Research*, v. 90, p. 11,319–11,333.
- Mainprice, D., 1990, A FORTRAN program to calculate seismic anisotropy from the lattice preferred orientation of minerals: *Computers & Geosciences*, v. 16, p. 385–393.
- Mehl, L., Hacker, B.R., and Hirth, G., 2003, Arc-parallel flow within the mantle wedge: Evidence from the accreted Talkeetna arc, south central Alaska: *Journal of Geophysical Research*, v. 108, no. B8, 2375, doi: 10.1029/2002JB002233.
- Mercier, J.-C.C., 1985, Olivine and pyroxenes, in Wenk, H.-R., ed., *Preferred orientation in deformed metals and rocks: Introduction to modern texture analysis*: Orlando, Florida, Academic Press, p. 407–433.
- Mizukami, T., Simon, W., and Yamamoto, J., 2004, Natural examples of olivine lattice preferred orientation patterns with a flow-normal *a*-axis maximum: *Nature*, v. 427, p. 432–436.
- Möckel, J.R., 1969, Structural petrology of the garnet peridotite of Alpe Arami (Ticino, Switzerland): *Leidsche Geologische Mededelingen*, v. 42, p. 61–130.
- Nicolas, A., and Christensen, N.I., 1987, Formation of anisotropy in upper mantle peridotites—A review, in Fuchs, K., and Froideveaux, C., eds., *Composition, structure and dynamics of the lithosphere-asthenosphere system*: Washington, D.C., American Geophysical Union, p. 407–433.
- Paterson, M.S., 1982, The determination of hydroxyl by infrared absorption in quartz, silicate glasses and similar materials: *Bulletin de Mineralogie*, v. 105, p. 20–29.
- Sawaguchi, T., 2004, Deformation history and exhumation process of the Horoman peridotite complex, Hokkaido, Japan: *Tectonophysics*, v. 379, p. 109–126.
- Tanimoto, T., and Anderson, D.L., 1984, Mapping convection in the mantle: *Geophysical Research Letters*, v. 11, p. 287–290.
- Zhang, S., and Karato, S., 1995, Lattice preferred orientation of olivine aggregates deformed in simple shear: *Nature*, v. 375, p. 774–777.

Manuscript received 5 May 2004

Revised manuscript received 3 September 2004

Manuscript accepted 8 September 2004

Printed in USA